Journal of Analytical and Applied Pyrolysis 177 (2024) 106341

Contents lists available at ScienceDirect

Journal of Analytical and Applied Pyrolysis

journal homepage: www.elsevier.com/locate/jaap

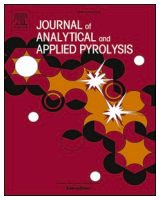

Optimization of waste cork powder torrefaction to improve biofuel parameters and storage properties

Belén Escribano-Uriarte, Lorena Pérez-Carcelén, José Antonio Díaz-López *, Evangelina Atanes-Sánchez

Universidad Politécnica de Madrid (UPM), Department of Mechanical, Chemical and Industrial Design Engineering, ETSIDI, 28012 Madrid, Spain

ARTICLE INFO

Keywords:
Biomass
Torrefaction
Factorial design
Thermogravimetric analysis
Waste cork
Renewable energy

ABSTRACT

Waste cork torrefaction was optimized in order to improve the properties of this material for its application as biofuel. A two-level factorial design involving three factors -torrefaction temperature, torrefaction time and heating rate- was proposed with two-responses -mass yield (MY) and high heating value (HHV)-. Factorial design results revealed that torrefaction time and especially temperature were the most influential factors. Using simultaneous optimization of the two variables MY and HHV, and giving them two different weights, two different sets of optimum conditions were obtained. The first one (246 ºC, 60 min and 5 ºC/min) led to a biofuel with similar HHV as the raw material, therefore it did not give any benefit in terms of biofuel upgrading. The second one (275 ºC, 60 min and 5 ºC/min) gave a biofuel with 10% more energy density than the raw material, which allowed to classify this biofuel as lignite. Both torrefied samples showed significant increase in hydrophobic character. Finally, ATR-FTIR results revealed the occurrence of carbonization reactions during torrefaction.

1. Introduction

Nowadays, several warnings coming from different points support strongly the urgent need of moving energy supply from fossil fuel to renewable sources. Among them, it stands the Sixth Assessment Report of the IPCC [1], which asserts that climate change has already caused substantial damages, and increasingly irreversible losses in terrestrial, freshwater, coastal and ocean ecosystems. These effects are mainly caused by greenhouse gas emissions, which have increased steadily since the early 20th century. Although important efforts have been made to face this issue, the crude reality is that around 80% of World total energy supply still comes from fossil fuels (coal, oil, natural gas) [2]. Last but not least, recent events have revealed that fossil fuels are dependent on geopolitical events that provoke insecurity in energy supply and cost.

Among renewable sources, biomass shows characteristics that make interesting the promotion of its use in combination with other renewable sources. On one hand, energy supply from biomass is manageable, so that it can be used to support intermittent energy sources, such as wind or solar photovoltaic, in those moments in which they cannot satisfy all the energy demand. On the other hand, the use of biomass can reduce the dependence of some countries on other ones and therefore alleviate the geopolitical issues above mentioned. Additional benefits arise if waste biomass is used, such as to prevent the exploitation of natural biomass (*natural CO_2 sinks*) and other issues such as fire hazard or landfilling.

However, the use of biomass as energy source presents some bottlenecks that many times limit its use at commercial scale. Among them, it stands the low HHV (16–20 MJ/kg) [3] respect to coal-based counterparts (up to 30–34 MJ/kg) [4], which hinder the economic viability of biomass energy use. Besides, the high water content of biomass, together with the low density, resulted in additional transport and storage issues.

In this sense, torrefaction of biomass emerges as a potential upgrading process that allows to improve the fuel properties above mentioned. Torrefaction, also known as mild pyrolysis, consists on heating biomass up to 200–300 ºC under inert atmosphere, usually nitrogen. Biomass torrefaction is not just a sometimes so-called *strong drying* process, but allows to increase the energy density of the biofuel by removing moisture and the less energy-valuable volatile fractions [5]. Besides, it has been reported that torrefaction increase biomass hydrophobicity and grindability, which affected directly to transport, storage and particle size reduction costs [6].

Torrefaction of different types of waste biomass has been reported in the literature. Among the most recent publications, Brojolall et al. [7]

* Corresponding author.
E-mail address: jose.dlopez@upm.es (J.A. Díaz-López).

https://doi.org/10.1016/j.jaap.2023.106341
Received 2 January 2023; Received in revised form 30 October 2023; Accepted 29 December 2023
Available online 6 January 2024

Nomenclature

Symbol	description
M	mass (mg)
T	torrefaction time (min)
T	torrefaction temperature (°C)
X_T	temperature coded factor
X_t	torrefaction time coded factor
X_{HR}	heating rate coded factor
HR	heating rate (°C/min)
db	dry basis
wb	wet basis
MY	mass yield (%)
EY	energy yield (%)
FR	fuel ratio
E_D	energy density
FC	fixed carbon content (%)
VM	volatile matter content (%)
HHV	higher heating value (MJ/kg)
TGA	thermogravimetric analysis
DTG	derivative thermogravimetry
Ti	ignition temperature (ºC)
Tp	peak temperature (ºC)
Tb	Burnout temperature (ºC)
S	combustion index
α_{Ti}	fraction of material degraded at Ti (%)
α_{Tb}	fraction of material degraded at Tb (%)
EMC	equilibrium Moisture Content (%)

analysed the effect of torrefaction of bagasse, corn stalk and leaves and coconut shell on their fuel properties. To this end, they studied the effect of torrefaction time, temperature and particle size using a cylindrical batch reactor. The authors conclude that the highest HHV (25.9 MJ/kg) was achieved at the most severe conditions (300 ºC, 60 min) and using the highest particle size (0.9 mm). Abdullah et al. [8] explored the potential benefits of the torrefaction of biomass blends, specifically, walnut shell and pearl millet. They also analysed the effect of torrefaction temperature and time. The main conclusion was that torrefaction at 260 ºC and 30 min, using a blend consisting of 70% pearl millet and 30% walnut shell, reached a HHV of 27 MJ/kg. Finally, Cardarelli et al. [9] studied the effect of torrefaction temperature on the thermal behaviour of spent coffee grounds under combustion conditions, with the aim of comparing the kinetics, combustion performance and thermodynamics of raw and torrefied spent coffee grounds. The main conclusions of this work were, on the one hand, that sample torrefied at 235 ºC showed the highest combustion index, and on the other hand, that torrefaction of spent coffee grounds at 235 and 260 ºC was suitable to produce biofuel with improved combustion characteristics. Previously, many studies concerning torrefaction of different sources of lignocellulosic biomass have been reported in the literature. An overview of these works has been included in an excellent recent review reported by Sarker et al. [10].

In this work, torrefaction of waste cork powder was analysed. Cork powder is the main residue of cork industry, being generated throughout all the fabrication stages of cork-based product manufacturing and representing up to 30% of the raw material [11]. Regarding waste cork powder torrefaction, literature is very scarce. As far as the authors are concerned, there are only three works related to this issue, two of them reported by Sen et al. In the first one [12], they studied low pyrolysis of waste cork at 200, 250, 300 and 350 ºC, and analyze fuel properties (together with leaching and adsorption ones). The main conclusion they draw was that cork-derived biochar torrefied above 300 ºC showed lignite and coal-like composition. In their second study [13], they focused on analysing liquid and gas products. The main finding was that guaiacol was the main condensate product, whereas CO_2 was the main gas one. Finally, a previous study of Lee et al. [14] analysed waste cork torrefaction, but on the basis of implementing this process as pretreatment prior to waste cork pyrolysis. The purpose of this work is to optimize waste cork powder torrefaction to obtain upgraded biofuel, on the basis of mass and energy parameters. Optimized conditions were then tested at bench-scale, in order to analyze in detail biofuel combustion and storage properties. The authors of the present work consider the achievements of this work will suppose a breakthrough in the valorization of waste cork powder as biofuel.

2. Materials and methods

2.1. Materials

The present study has selected a second-generation biomass type: waste cork powder *(Quercus suber)* from Sanvicork S.A. located in San Vicente de Alcántara (Badajoz, Spain), with a bulk density of 291.85 kg/m^3. Table 2–1 lists the particle size distribution of the sample:

2.2. Design of experiments

The torrefaction process was studied and optimised following the factorial design and response surface methodology in order to save time and resources [15,16]. A two-level (2^k) factorial design has been carried out to evaluate the torrefaction process, involving three factors (k = 3) each one at low and high level.

Selection of factors and levels was based on the operating conditions that have a significant influence on the torrefaction process, according to the literature and previous experiences. The factors and levels were the following: final torrefaction temperature with lower level at 230 °C and upper level at 300 °C; torrefaction time, i.e., the time during which sample is submitted to final torrefaction temperature, with lower level at 30 min and upper level at 60 min; and heating rate with lower level at 5 °C/min and upper level at 15 °C/min. Therefore, the design consisted of 2^k experiments (i.e. 8 experiments in this case) corresponding to every possible combination of these factors. Additionally, 6 repeated experiments in the center point of the range of each factor (265 °C, 45 min, 10 °C/min) were added to evaluate the deviation of the results. It is important to highlight that center point experiments do not belong to factorial design. The experiments were conducted randomly to minimize errors due to possible systematic trends in the variables.

Two responses with opposite trends were selected: the mass yield (MY), which reaches the maximum at the softest torrefaction conditions, and the higher heating value (HHV), which increases along with the severity of torrefaction conditions. These two responses were selected to reach a compromise on the optimum conditions: the goal was to enhance

Table 2–1
Particle size distribution of the waste cork powder used in this study.

Mesh (mm)	Sample percentage (%)
3	1.03
2	2.97
1	13.16
0.8	5.03
0.5	14.42
0.3	22.88
0	40.50

biomass energy properties preventing an excessive mass loss at the same time. A two-response optimization method was chosen as reported by several authors [17,18].

The standard experimental matrix for the factorial design is shown in Table 3–1. Columns 2, 3 and 4 represent the factor levels on a natural scale, and columns 5, 6 and 7 represent the 0 and ± 1 encoded factors levels in a dimensionless scale. The first 8 lines correspond to the experimental design and the last 6 lines to the central point. Table 3–1 also shows the experimental results of the two selected responses in columns 8 and 9.

A statistical analysis was carried out with these experimental values, and the main effects and interaction effects of the variables were calculated for the two responses variables. ANOVA was performed to understand the fitness and statistical significance of the regression models. Experimental results were fitted to a linear mathematical model to predict the response in the experimental region and to locate the optimum conditions.

For the simultaneous optimization of the two response variables, the model proposed by Derringer and Suich was followed [19], transforming the response into a desirability function, which can be optimized by univariate techniques. The whole statistical analysis was performed using Statgraphics software *(v.18, Statgraphics Technologies Inc.)*.

2.3. Torrefaction and proximate analysis

The torrefaction process was carried out in a thermogravimetric analyser (*TGA SDT Q600, TA Instruments*). Several temperatures were investigated (230 - 300 °C) under a nitrogen atmosphere (Air Liquide, Alphagaz ≥ 99.999%) at a constant flow rate of 60 NmL/min. Related to Fig. 2–1, each sample (around 20 mg) was placed in a platinum sample pan and first dried at 105 °C for 20 min (a). Subsequently the samples were heated at different rates (from 5 to 15 °C/min) up to the set torrefaction temperature (b), which was maintained between 30 and 60 min (c). After torrefaction, the furnace cooled down to 60 °C (d) spontaneously in the same atmosphere. A proximate analysis was also performed in the same experiment following the procedure described in the TA Instrument Technical Note [20] based in the applicable standards [21–23]. Right after the torrefaction process, the sample was heated up to 200 °C at a rate of 15 °C/min and remained at that temperature for 5 min (e). Afterwards, it was heated up to 900 °C (f), still under an inert atmosphere, and held for 10 min. Then the atmosphere gas switched from nitrogen to oxygen (Air Liquide, Alphagaz ≥ 99.995%) (g) and the temperature was held for 15 min. Finally, the sample was cooled down to room temperature. The process was computer controlled with the data recorded to the hard drive for future analysis through the TGA and DTG curves.

Table 3–1
Experiment matrix design and experimental results: factorial and central points. X: coded value. T: temperature. t: torrefaction time; HR: heating rate.

Run	T (°C)	t (min)	HR (°C/min)	X_T	X_t	X_{HR}	MY (%)	HHV (MJ/kg)
1	230	30	5	-1	-1	-1	89.32	19.32
2	300	30	5	+1	-1	-1	64.92	21.53
3	230	60	5	-1	+1	-1	85.55	20.35
4	300	60	5	+1	+1	-1	59.01	22.06
5	230	30	15	-1	-1	+1	90.82	19.15
6	300	30	15	+1	-1	+1	66.08	21.41
7	230	60	15	-1	+1	+1	88.53	19.12
8	300	60	15	+1	+1	+1	59.23	22.14
9	265	45	10	0	0	0	76.61	21.16
10	265	45	10	0	0	0	77.68	20.3
11	265	45	10	0	0	0	76.81	20.99
12	265	45	10	0	0	0	76.61	20.69
13	265	45	10	0	0	0	77.11	20.32
14	265	45	10	0	0	0	77.27	20.77

The proximate analysis provided data to evaluate the volatile matter (VM) and ash content. The fixed carbon (FC) content was obtained through the subtraction between the 100% and the former components, as described in Eq. (1), where all parameters are given in dry basis:

$$FC_{db} = 100 - VM_{db} - ASH_{db} \quad (1)$$

This whole procedure was applied to three samples of as-received waste cork powder. The following mean values were obtained: 8.52% moisture (wet basis), 74.71% volatile matter (dry basis), 3.83% ash (dry basis) and therefore 21.91% fixed carbon (dry basis). The mean calculated HHV was 19.27 MJ/kg. Finally, the fuel ratio of as-received waste cork powder was 29.33%.

2.4. Evaluation of the torrefaction process

Torrefaction was evaluated through several mass and energy parameters calculated with data obtained in thermogravimetrical analysis and proximate analysis, such as:

The mass yield (MY) of the process, defined in Eq. (2) [24] as the ratio between the mass of the torrefied product and the raw biomass, both in dry basis.

$$MY(\%) = \frac{m_{torrefied\quad biomass(db)}}{m_{raw\quad biomass(db)}} \bullet 100 \quad (2)$$

The energy yield (EY), defined in Eq. (3) [24] as the energy content in the torrefied product.

$$EY(\%) = MY \bullet \frac{HHV_{torrefied\quad biomass}}{HHV_{raw\quad biomass}} \bullet 100 \quad (3)$$

The higher heating value (HHV) was estimated through a correlation proposed by Parikh *et. al* using the proximate analysis results (Eq. (4) [25]).

$$HHV(MJ/kg) = 0.3536 \bullet FC_{db}(\%) + 0.1559 \bullet VM_{db}(\%) - 0.0078 \bullet ASH_{db}(\%) \quad (4)$$

The energy density (E_D) defined in Eq. (5) [26], evaluates the increase in the energy content of the solid product.

$$E_D = \frac{EY}{MY} \quad (5)$$

The fuel ratio (FR), which evaluates the ratio between the FC and VM content in Eq. (6).

$$FR = \frac{FC_{db}}{VM_{db}} \quad (6)$$

2.5. Bench-scale torrefaction and biofuel characterization

Once the optimum torrefaction conditions have been set, bench scale experiments were conducted in a C610 alumina tube (5 cm i.d., 6 cm o.u., 5 W/mK) located in a horizontal furnace (ENERGON HLT 18–50-14) electrically heated. The S-type thermocouple of the furnace was located in the outer wall of the reactor, so temperature gradient caused by heat conduction through reactor wall (approximately 10 ºC) was considered for setting process temperature. Approximately, 1 g of cork powder waste, previously dried at 105 ºC for 24 h, was placed in a ceramic crucible in the center of the tube, then heated from room temperature to the optimum temperature at the optimum heating rate under continuous N_2 flow of 100 NmL/min. Sample was kept at that temperature for the optimum torrefaction time. Finally, sample was allowed to return to room temperature under the same flow, in order to protect biofuel from undesired oxidation. Sample then was weighted and stored for further characterization.

Characterization of the biofuel obtained at bench scale in the optimized experimental conditions can be divided into four main blocks. The first block corresponds to biofuel characterization. Proximate

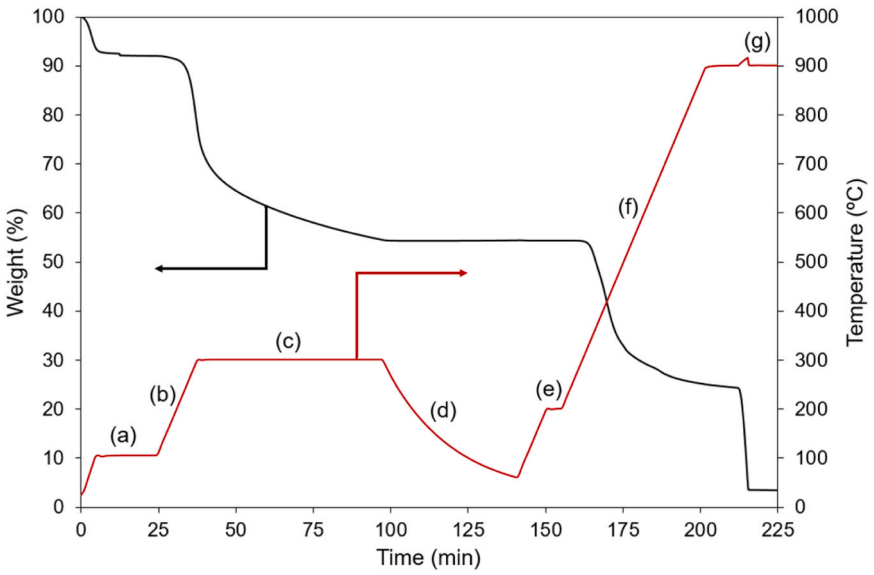

Fig. 2–1. Temperature and weight change in an experiment of torrefaction and proximate analysis carried out in series. Conditions: 300 °C, 60 min, 15 °C/min.

analysis was performed, using the equipment and experimental procedure above mentioned. The elemental content of carbon, hydrogen, nitrogen and sulphur was performed following the UNE-EN ISO 16948:2015 standard. For this purpose, a LECO CHNS 628 analyzer was used. The High Heating Value was determined following the UNE-EN ISO 14918:2011 standard, by using a PARR 6400 Automatic Isoperibol Calorimeter. Outcomes of these experiments were used to calculate the torrefaction parameters above mentioned in point 2.4. and evaluate the whole bench scale torrefaction process.

In the second characterization block, Fourier Transform Infrared Spectroscopy with Attenuated Total Reflectance (ATR-FTIR) was performed to study the chemical structure of the samples. A Perkin Elmer Frontier spectrometer equipped with a Universal ATR was used. Samples were sieved to particle diameter ≤ 300 μm, then placed on the diamond/ZnSe crystal of the ATR. Spectra were collected over 4000–650 cm^{-1}, with a resolution of 4 cm^{-1} and 15 scans per sample. For the sake of reproducibility, each sample was analyzed a minimum of six times.

In the third characterization block, biofuel combustion parameters were evaluated, following the procedure described by [9]. To this end, thermogravimetric analysis were performed under air atmosphere (100 NmL/min), from room temperature to 900 ºC, using a heating rate of 10 ºC/min. Approximately, 20 mg of sample were used in each run. Using derivative thermogravimetric results (DTG), the ignition temperature (T_i (ºC), temperature at which the weight loss rate is 1%/min after the initial weight loss caused by drying), the burnout temperature (T_b (ºC), temperature at which the burning rate reached 1%/min at the end of the DTG curve), the peak temperature (T_p (ºC), temperature at which the highest weight loss rate was achieved) and the combustion index (S) were computed (Eqs. (7) and (8)):

$$S = \frac{DTG_{\max}\left(\frac{\%}{\min}\right) DTG_{mean}\left(\frac{\%}{\min}\right)}{T_i^2 T_b} \tag{7}$$

$$DTG_{mean} = \frac{\alpha_{T_b} - \alpha_{T_i}}{(T_b - T_i)/HR} \tag{8}$$

Where α_{T_b} and α_{T_i} (%) are the fractions of material degraded at the burnout and ignition temperature, respectively, and HR is the heating rate.

The last block corresponds to hydrophobicity tests, for which the Equilibrium Moisture Content (EMC), previously reported [10], was performed. A Weiss Technik WKL 34/40 environmental chamber was used. Samples were previously dried in an oven for 24 h at 110 ºC, then weighted and sent to the environmental chamber, in which the environment conditions were set as 25 ºC and 85% relative humidity. After 24 h, samples were considered to be in equilibrium with the environment, so they were taken from the oven and weighted again, in order to evaluate the amount of water they absorbed. Data obtained allowed to quantify the hydrophobicity of samples studied.

3. Results and discussion

3.1. Results of factorial design

Table 3–1 presents the experimental matrix design including the results of response variables MY and HHV. Table 3–2 shows the main effects and the interaction effects of the factors for the response variables.

As can be observed in Table 3–2, the main effects showed opposite signs for both responses, meaning that factors have antagonistic effect on the two responses variables. Temperature was the most important factor, followed by the torrefaction time and heating rate, which has also been reported elsewhere for other biomass sources [27]. In this sense, increasing the temperature causes that the MY decrease in 26.24% due to the higher mass loss, whereas the HHV value increase in 2.3 MJ/kg due to the higher content in fixed carbon. The ANOVA analysis is presented in Tables 3–3 and 3–4 for MY and HHV variables respectively.

According to ANOVA analysis, those effects and interactions with F-value higher than 1 are significant. Moreover, the p-value is related to the confidence level, and a p-value less than 0.05 indicates that this main factor or interaction has statistical significance with a 95% confidence level. Therefore, Table 3–3. shows that, in the case of MY, just the temperature and torrefaction time were significant at 95% of confidence level, being the temperature more significant. The interaction

Table 3–2
Main effects and interactions for the two response variables (MY and HHV).

Main effects and interactions	MY (%)	HHV (MJ/Kg)
T: Temperature	-26.245	2.3
t: time	-4.705	0.565
HR: Heating rate	1.465	-0.36
T-t	-1.675	0.065
T-HR	-0.775	0.34
t-HR	0.135	-0.215

Table 3–3
ANOVA analysis for MY.

Source	Sum of squares	DF	Mean square	F-value	p-value
T	1377.6	1	1377.6	944.99	0.0000
T	44.274	1	44.274	30.37	0.0009
HR	4.29245	1	4.29245	2.94	0.1299
T-t	5.61125	1	5.61125	3.85	0.0906
T-HR	1.20125	1	1.20125	0.82	0.3942
t-HR	0.03645	1	0.03645	0.03	0.8788
Error total	10.2046	7	1.4578		
Total (corr.)	1443.22	13			

$R^2 = 99.2929\%$.

Table 3–4
ANOVA analysis for HHV.

Source	Sum of squares	DF	Mean square	F-value	p-value
T	10.58	1	10.58	90.30	0.0000
T	0.63845	1	0.63845	5.45	0.0523
HR	0.2592	1	0.2592	2.21	0.1805
T-t	0.00845	1	0.00845	0.07	0.7960
T-HR	0.2312	1	0.2312	1.97	0.2029
t-HR	0.09245	1	0.09245	0.79	0.4039
Error total	0.8202	7	0.117171		
Total (corr.)	12.63	13			

$R^2 = 93.5059\%$.

temperature-torrefaction time was significant with a 90% confidence level.

As for HHV, the ANOVA analysis of Table 3–4 shows that just the temperature was significant at 95% of confidence level. Torrefaction time was significant at 94.77% confidence level, so that it was considered significant in this work.

Experimental results of MY and HHV were fitted to a linear model that relates the response variables with the factors and the interactions between them and allow to estimate the value of the variables in the experimental range studied. Taking into account the significant coefficients (Tables 3–3 and 3–4), the following equations and regression coefficients were obtained using coded factors:

$$MY(\%) = 76.1107 - 13.1225 \bullet X_T - 2.3525 \bullet X_t (R^2 = 0.993) \quad (9)$$

$$HHV(MJ/kg) = 20.665 + 1.15 \bullet X_T + 0.2825 \bullet X_t (R^2 = 0.935) \quad (10)$$

Fig. 3–2 represents the predicted values calculated with Eqs. (9) and (10) versus experimental data, which helps to evaluate the adequacy of the mathematical models proposed in this study. As it is seen, most of data points lie very close to the diagonal, suggesting that there was good agreement between the model and the experimental data. The R^2 value was close to 1 in both cases, suggesting that the developed models are able to satisfactorily predict the value of MY and HHV.

Figs. 3–3 and 3–4 present the surface response of both variables MY and HHV obtained with the model Eqs. (9) and (10), respectively.

With this individual analysis for each response variable, the optimum MY of 91.8% was achieved for the softer torrefaction conditions of 230 °C, 30 min and 15 °C/min, whereas the HHV found the optimum value of 22.25 MJ/kg at the more severe conditions of 300 °C, 60 min and 5 °C /min. This result indicates that operating conditions for these two responses variables should be a compromise between the improvement of HHV without a drastic reduction of MY, as a high

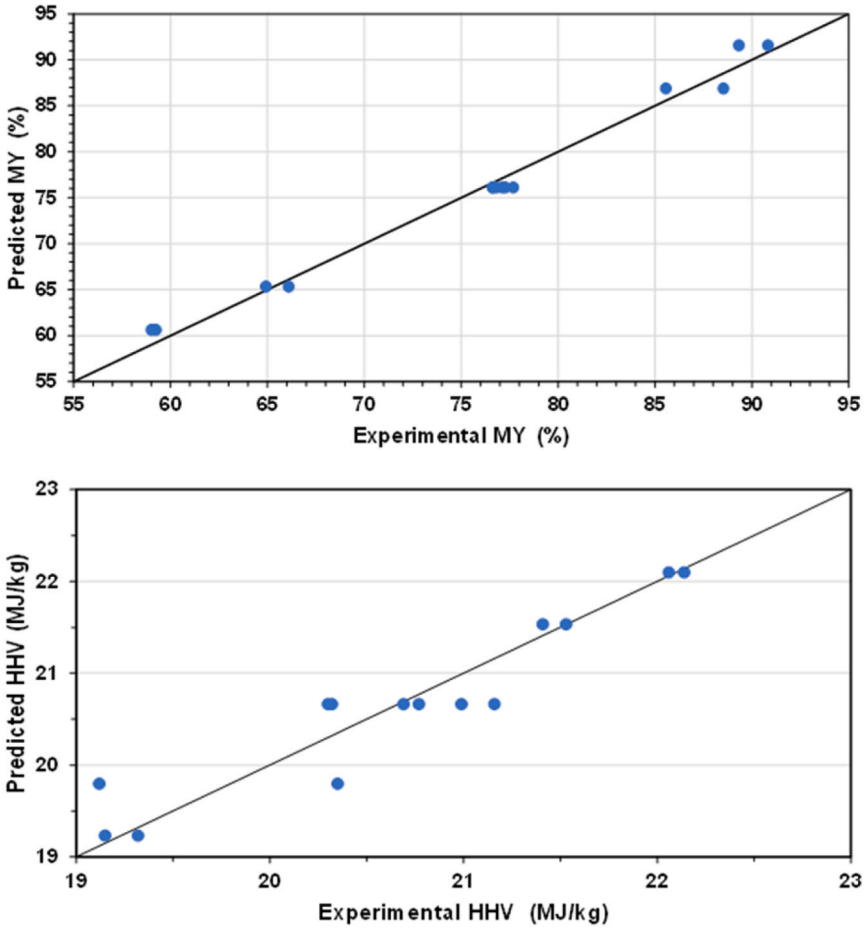

Fig. 3–2. Experimental results vs. model predicted values for MY (top) and HHV (bottom).

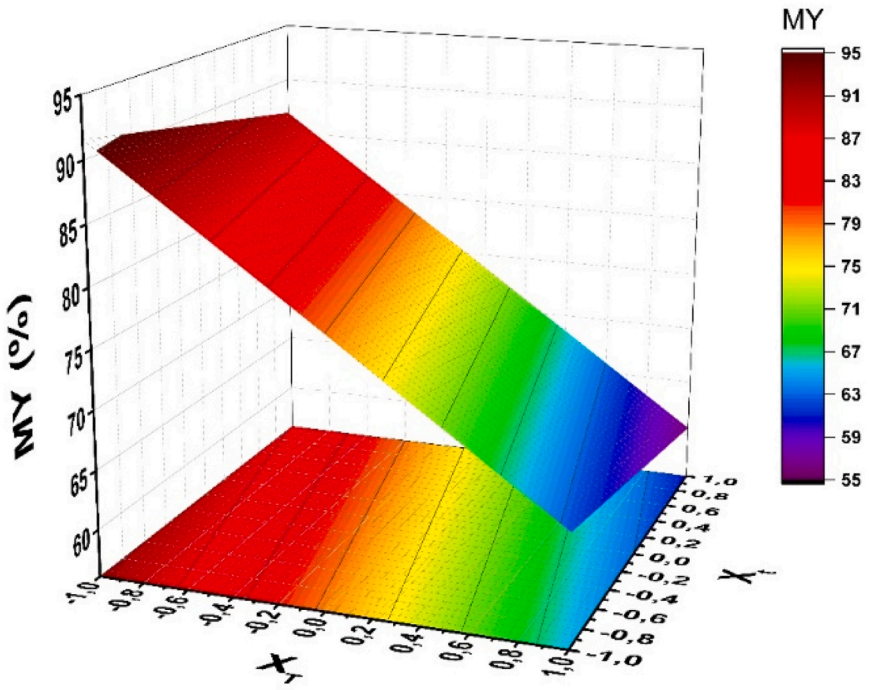

Fig. 3–3. Surface response for MY.

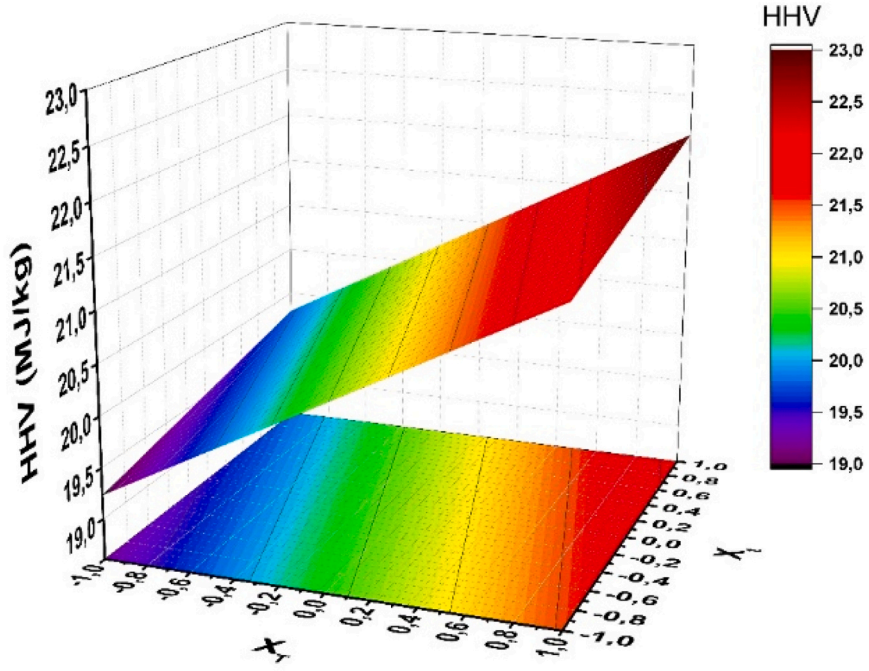

Fig. 3–4. Surface response for HHV.

quality fuel is pursued but minimizing the mass loss.

3.2. Simultaneous optimization of the two response variables MY and HHV

Due to the opposite trend observed for both response variables with the studied factors, a simultaneous optimization employing the Derringer's desirability method was carried out. Equal weight (50%–50%) was given to MY and HHV. The optimal operating conditions were a temperature of 246 °C, a torrefaction time of 60 min and a heating rate of 5 °C/min. This optimal point corresponds to a MY value of 80.14% and a HHV value of 20.7 MJ/Kg, that means an increase of 7.4% in HHV with respect to the initial cork waste. The desirability value was of 58.96%, similar to that obtained by other authors. In this sense, in the torrefaction of pigeon pea stalk, a desirability of 54% was obtained for the simultaneous optimization of energy yield and HHV [18], whereas a desirability between 52.1–56.2% was the result for the simultaneous optimization of HHV and mass loss in the torrefaction of coffee industry waste [17].

Looking for operating conditions that favor increasing the HHV

values, a simultaneous optimization giving higher weight to HHV was conducted, specifically 75% weight for HHV and 25% weight for MY. In this case, the optimal point corresponded to a temperature torrefaction of 275 °C, with the same values of time torrefaction and heating rate at 60 min and 5 °C/min, respectively. In this point, a MY of 69.5% and a HHV value of 21.5 MJ/kg were obtained, that implies an increase of 11.6% of HHV compared to the initial cork waste. In this case, the desirability value was of 63.15%, which suppose higher desirability of the corresponding response than that of the previous optimization. This higher desirability should be regarded in terms of statistics, and the biofuel properties should be analyzed in detail after thorough characterization.

3.3. Scale-up of the torrefaction process

Once determined the optimal torrefaction operating conditions, a series of experiments were conducted in these conditions both at lab scale (torrefaction at TGA equipment in series with proximate analysis at TGA) and at bench scale (torrefaction at tubular reactor and proximate analysis at TGA), with the aim of evaluating the scale-up of the torrefaction process.

Table 3–5 presents the results of several mass and energy torrefaction parameters. These results allow to compare, on the one hand, the bench scale and laboratory scale, and on the other hand, the bench scale and the results predicted by the mathematical models. Bench scale experiments were repeated three times, and the relative standard deviation in all cases was less than 1%.

Torrefaction parameters of these experiments (Table 3–5) were similar as those obtained by thermogravimetric analyses, which allowed to validate these experiments prior to biofuel characterization. Considering the scale-up from TGA to tubular reactor, and for the two set of optimal conditions, the deviations for MY values where higher than that of HHV values. All deviations increased with temperature, which can be ascribed to higher thermal gradients inside the tubular reaction at higher operation temperature. In any case, the maximum deviation was less than 10%. The same trend was observed for the comparison between the bench scale results and the values predicted by the model. Deviation values fell below 12%, which allow to conclude that the developed mathematical model was adequate for scaling-up the torrefaction of waste cork.

Table 3–5
Comparison of results between laboratory scale torrefaction, bench scale torrefaction and mathematical models.

		MY (%)	HHV (MJ/kg)[1]	EY (%)	E^2_{Dtheo}
Opt1 (246 °C, 60 min, 5 °C/min)	Laboratory scale (TGA)	84.05	19.91	86.85	1.03
	Bench scale	85.37	20.09	88.98	1.04
	Model predicted value	80.88	20.32	85.30	1.05
	Deviation (%) Bench scale – TGA	1.56	0.88	2.46	0.88
	Deviation (%) Bench scale – Predicted	5.54	-1.17	4.31	-1.17
Opt2 (275 °C, 60 min, 5 °C/min)	Laboratory scale (TGA)	71.30	20.81	76.99	1.08
	Bench scale	77.99	20.19	81.73	1.05
	Model predicted value	70.01	21.28	77.30	1.10
	Deviation (%) Bench scale – TGA	9.38	-2.95	6.16	-2.95
	Deviation (%) Bench scale – Predicted	11.40	-5.09	5.73	-5.09

[1] $HHV\left(\frac{MJ}{kg}\right) = 0,3536 \cdot FC_{db} + 0,1559 \cdot VM_{db} - 0,0078 \cdot ASH_{db}$

[2] Energy density using HHV obtained by mathematical correlation

3.4. Bench-scale torrefaction

Torrefied biofuels at both optimum conditions were characterized by different techniques. Table 3–6 lists biofuel characterization results along with the properties of as received cork powder. It is important to point out that proximate analyses were conducted after several weeks, in order to let torrefied samples to reabsorb moisture from ambient air. First of all, proximate analysis results revealed that torrefaction, at first sight, led to a more hydrophobic biofuel, as later observed by EMC experiments (see hereafter). Volatile matter also showed a slight decrease, which was more pronounced as torrefaction temperature was higher. This decrease was associated to the thermal degradation of hemicellulose fraction, as reported previously for cork samples [28,29] and other lignocellulosic biomass samples [30,31]. To confirm this fact, DTG results of samples torrefied at different temperatures are shown in Fig. 3–5. These results confirmed that the first DTG peak (295 ºC), which can be associated to hemicellulose fraction [32], vanished as torrefaction temperature increased. As expected, this volatile matter decreases derived in an increase of fixed carbon and ash content. However, ash content results obtained in the sample torrefied at 246 ºC were not completely conclusive, as it was expected an increase respect to those of as-received cork powder. Consequently, the fuel ratio of torrefied samples was higher than that of the raw material.

Ultimate analysis results showed that elemental carbon content increased and oxygen content decreased, whereas the content of the rest of elements remained practically constant. The reduction of oxygen content can be ascribed to hemicellulose removal. It is accepted that hemicellulose is composed of pentoses ($C_5H_{10}O_5$) and hexoses ($C_6H_{12}O_6$), in which the oxygen and hydrogen content is higher than that of cellulose (typically $C_6H_{10}O_5$) and especially lignin ($C_{10}H_{15}O_3$) [33]. Therefore, hemicellulose removal resulted in higher oxygen and hydrogen removal than carbon removal, so that the percentage of elemental carbon was higher on torrefied samples. It should not be discarded the occurrence of secondary reactions such as depolymerisation, recondensation, deoxygenation or carbonization [10]. ATR-FTIR analyses try to shed some light about this issue (see hereafter).

Using elemental analysis results, it was possible to compute the oxygen to carbon and hydrogen to carbon ratios, which are parameters

Table 3–6
Biofuel characterization results.

		As-received cork powder	Torrefied cork powder	
			246 °C, 60 min, 5 °C/min	275 °C, 60 min, 5 °C/min
Proximate analysis	**Moisture $(\%)_{wb}$**	8.52	4.96	5.07
	VM $(\%)_{db}$	74.71	72.53	68.32
	FC $(\%)_{db}$	21.91	23.71	27.21
	Ash $(\%)_{db}$	3.83	3.76	4.47
FR (%)		29.33	35.55	39.91
Ultimate analysis $(\%)_{db}$	**C**	55.20	57.24	62.78
	H	5.71	5.66	5.75
	N	1.01	0.95	1.06
	S	0.05	0.04	0.05
	O[1]	34.19	32.36	25.88
10•H/C		1.035	0.988	0.917
O/C		0.613	0.562	0.408
HHV[2] (MJ/kg)		21.28	21.26	23.30
E^3_{Dreal}		1.000	0.999	1.094

[1] $O_{db} = 100 - (C_{db} + H_{db} + N_{db} + S_{db} + A_{db})$

[2] Using UNE-EN ISO 14918:2011 standard

[3] Energy density obtained using bench-scale MY and experimental HHV

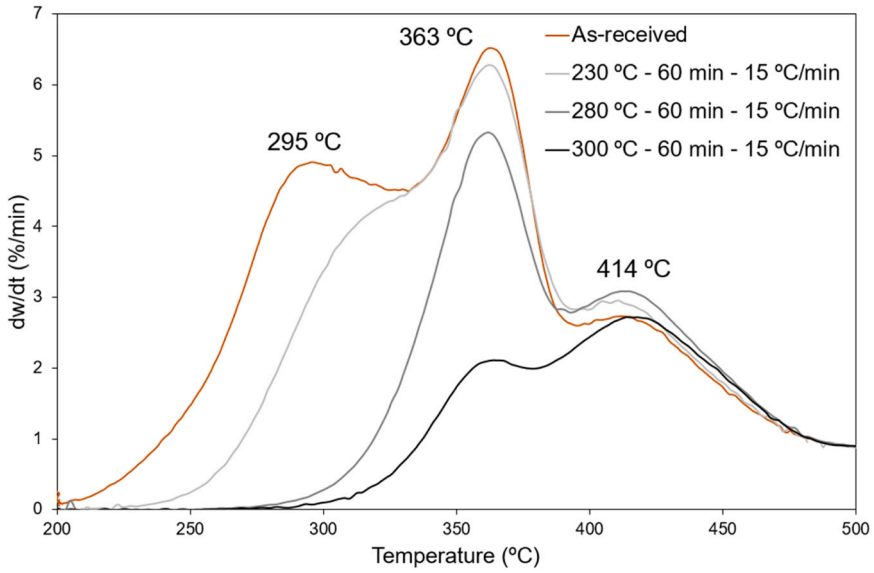

Fig. 3–5. DTG of as-received cork powder and torrefied samples heated from room temperature to 900 ºC under N_2 atmosphere.

that allow to compare biofuels and other solid fossil fuels through Van Krevelen diagram. According to one of the last publications in which this diagram is reported [34], torrefied cork powder samples, specially that sample torrefied at 275 ºC, fell into lignite area, confirming the benefit of this process in terms of biofuel classification and performance.

Finally, HHV experimental results showed differences respect to what was estimated by the correlation of Parikh et al. In this sense, sample torrefied at 246 ºC did not show any increase in HHV value, showing the same value as that of the as-received sample. On the other hand, sample torrefied at 275 ºC experienced a 10% increase of HHV, with the subsequent increase in energy density. Therefore, only torrefaction at the optimum obtained at higher temperature did result in a real increase in HHV, energy density and definitely an improved biofuel from waste cork powder.

In order to have a deeper understanding of the torrefaction process, ATR-FTIR analyses were carried out. Spectra of as-received cork powder and torrefied samples at optimum conditions are depicted in Fig. 3–6. A main absorption band at 1030 cm^{-1}, attributed to the stretching vibration of C-O bonds, was observed in all samples, which can be associated to the presence of polysaccharides [35,36]. This band was less intense as torrefaction conditions were more severe, which revealed the degradation of part of polysaccharides structure (probably hemicellulose and cellulose) during torrefaction process. Other bands that can be related to cellulose and hemicellulose (1154 and 1267 cm^{-1}) [37] were also observed, but there were no differences between as-received and torrefied samples. Conversely, higher absorption bands at 1319 (C-O of

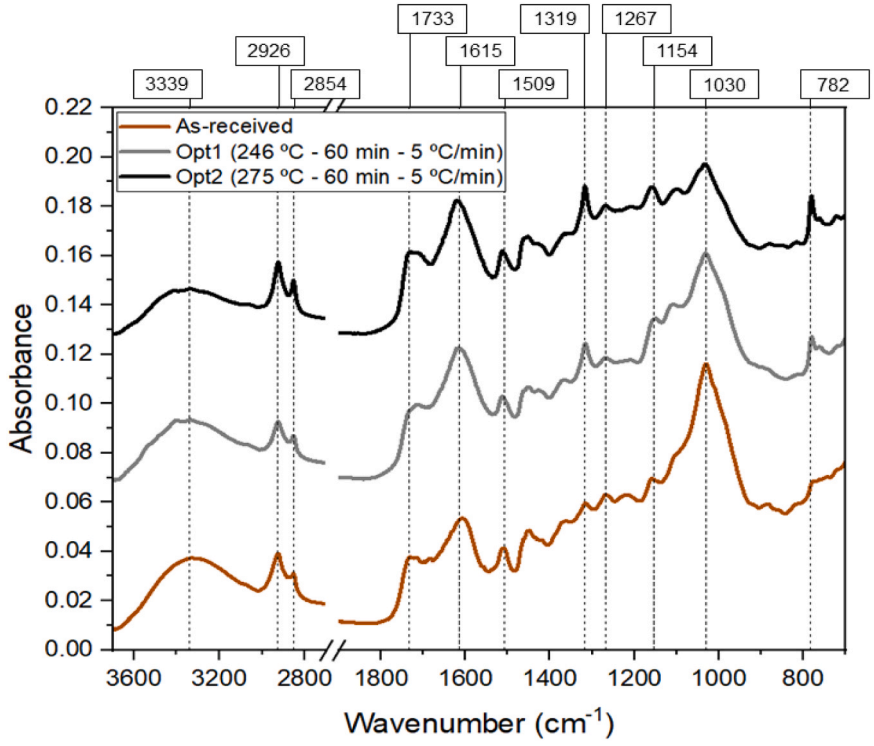

Fig. 3–6. ATR-FTIR spectra of as-received cork powder and torrefied samples at optimum conditions.

syringyl ring), 1509 (aromatic ring) and 1615 cm^{-1} (aromatic C═C), which can be associated to the presence of lignin [35,36,38], were observed at higher torrefaction temperatures, confirming the stability of lignin against torrefaction conditions.

Absorption bands at 2926, 2854 (stretching vibration of C-H) [39] and 1733 cm^{-1} (stretching vibrations of fatty acid ester (O-C═O)) were observed, which indicates the presence of suberin in all samples [35]. Therefore, it is possible to conclude that torrefaction did not cause suberin degradation in any case, in agreement to that reported by [35].

One of the most interesting absorption bands is the one that appeared at 782 cm^{-1} in torrefied samples. According to the literature [40], this band, together with the one at 1319 cm^{-1}, could appeared because of the increased content of asphaltene-like heterocyclic aromatic compounds, which may be linked to the occurrence of carbonization reactions during torrefaction process.

Last but not least, it was observed a broad absorption peak at around 3339 cm^{-1}, which corresponds to O-H stretching [41]. Regarding this broad peak, the higher the torrefaction temperature, the lower the peak height. Although it can also be ascribed to the reduction of hemicellulose and cellulose fractions [41], another plausible explanation is the reduction in adsorbed water in torrefied samples. This last fact can be related to higher hydrophobicity of torrefied samples, as confirmed by the EMC experiments later explained.

Table 3–7 shows the combustion and hydrophobicity parameters of raw and torrefied samples. Fig. 3–7 depicts the DTG curves of the samples studied. All samples showed two main peaks. The first one (320–340 ºC) is related to the maximum rate of volatile matter devolatilization, whereas the second one (402–409 ºC) is related to combustion of fixed carbon [42]. As-received cork powder showed an additional shoulder which, in agreement to previous result, can be ascribed to hemicellulose devolatilization. Combustion parameters were obtained on the basis of DTG results. First of all, it is observed that, the higher the torrefaction temperature, the higher the ignition temperature. This observation can be ascribed to hemicellulose removal, in agreement with biofuel characterization results. As reported previously [9], higher ignition temperature results in a thermally stable fuel and therefore more difficult to ignite. At the same time, biofuels with higher ignition temperature are safer for storage, as they are less likely to suffer spontaneous combustion in storage units. Concerning peak temperature, results of Table 3–7 revealed that there was practically no difference between samples. However, it was observed that, the higher the torrefaction temperature, the lower the variable DTG_{max} and the higher the T_b. As a consequence, combustion index (Eq. 7) was lower at higher torrefaction temperature, which allowed to conclude that torrefaction hinder biochar combustion. This fact can be ascribed to the deactivation of active sites or the volatilization of mineral catalysts [43].

Finally, important findings were obtained from EMC results. The first one was that the as-received material showed low EMC, so it can be classified as dry biomass. Nevertheless, experiments revealed how torrefaction can increase the hydrophobicity of the biofuel, as an important EMC reduction (up to 50%) was achieved. Comparing torrefied samples, it is possible to assert that, the higher the torrefaction temperature, the higher the hydrophobicity of the resulting material. According to [10], torrefaction causes depolymerisation reactions which result in the formation of non-polar molecules. In any case, further research is required to tackle this issue.

Table 3–7
Combustion and hydrophobicity parameters of raw and torrefied samples.

Sample	As-received cork powder	Torrefied cork powder	
		246 ºC, 60 min, 5 ºC/min	275 ºC, 60 min, 5 ºC/min
T_i (ºC)	235.9 ± 1.5	257.1 ± 1.2	268.3 ± 1.0
T_p (ºC)	412.3 ± 8.0	402.9 ± 2.2	406.1 ± 2.6
T_b (ºC)	433.1 ± 16.2	447.6 ± 22.3	449.5 ± 19.2
DTG_{max} (%/min)	20.1 ± 1.4	19.1 ± 2.2	18.0 ± 1.3
DTG_{mean} (%/min)	4.2	4.4	4.6
$S•10^6$	3.47	2.81	2.56
EMC $(\%)_{25ºC,\ 85\%\ RH,\ 24\ h}$	10.69 ± 0.44	6.32 ± 0.25	5.36 ± 0.29
EMC reduction (%)	-	40.91	49.85

4. Conclusions

The outcomes of this study allowed to draw the following conclusions:

- A two-level (2^k) factorial design has been applied to optimize the torrefaction process of waste cork powder. In the experimental range studied, and for a 95% of confidence level, the effects of temperature and time of torrefaction were significant in MY and HHV, being the temperature the most important factor.

- The simultaneous optimization of MY and HHV using the Derringer's desirability functions resulted in optimal operating conditions of 246 °C, 60 min and 5 °C/min for equal weight for MY and HHV, and 275 °C, 60 min and 5 ºC/min for 75% weight for HHV.

- The scale-up of the torrefaction process from the TGA tests to bench scale tests was carried out for these two optimum operating conditions, showing a close agreement between the results of MY and HHV obtained at lab scale and bench scale. These results indicated that equations model developed in TGA equipment allow to predict the operating conditions required for torrefaction test at bench scale to obtain a given value of these responses.

- During torrefaction process, removal of cellulose and especially hemicellulose took place. Lignin and suberin fractions did not suffer important changes. ATR-FTIR results showed the occurrence of carbonization reactions during torrefaction, as asphaltene-like heterocyclic aromatic absorption bands appeared in spectra of torrefied samples.

- Torrefaction at 246 ºC, 60 min and 5 ºC/min did not show important changes in terms of biofuel properties, as only a small decrease in volatile matter was observed, which can be ascribed to hemicellulose removal. These changes did not determine any increase in the HHV respect to that of the initial sample. The only benefit ascribed to torrefaction at these conditions was 40% less EMC at 25 ºC and 85% relative humidity for 24 h, so that these conditions should be ruled out for torrefaction scale-up.

- Torrefaction at 275 ºC, 60 min and 5 ºC/min resulted in a biofuel with 10% more HHV, which resulted in 10% more energy density than the raw material. On the other hand, the H/C and O/C ratios decreased, which allowed to classify this biofuel as lignite according to Van Krevelen diagram. Again, hemicellulose removal was the reason of these results. Conversely, combustion index of this material was lower than that of the raw material. Torrefied cork powder at 275 ºC, 60 min and 5 ºC/min resulted in a 50% more hydrophobic material, according to EMC results. Therefore, this set of optimum conditions is considered adequate for improving biofuel properties of waste cork powder.

CRediT authorship contribution statement

Belén Escribano-Uriarte: Writing – original draft, Methodology, Investigation, Formal analysis. **Lorena Pérez-Carcelén**: Methodology, Investigation, Formal analysis. **José Antonio Díaz-López**: Conceptualization, Writing – original draft, Investigation, Validation, Resources, Supervision. **Evangelina Atanes-Sánchez**: Conceptualization, Writing – original draft, Investigation, Validation, Resources, Supervision.

Declaration of Competing Interest

The authors declare that they have no known competing financial interests or personal relationships that could have appeared to influence

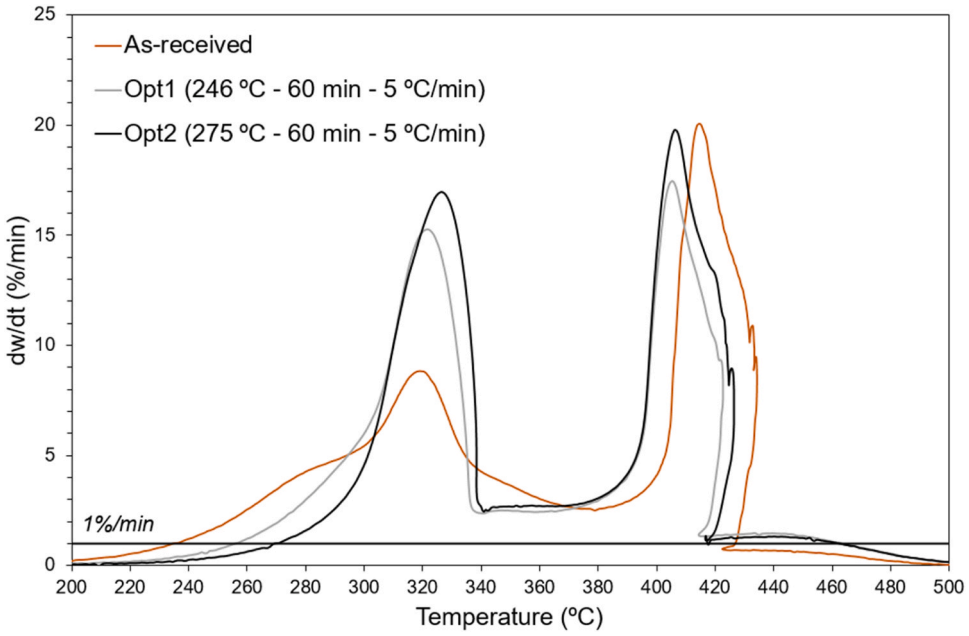

Fig. 3–7. DTG of as-received cork powder and torrefied samples at optimum conditions from room temperature to 900 ºC under air atmosphere.

the work reported in this paper.

Data availability

No data was used for the research described in the article.

References

[1] Intergovernmental Panel on Climate Change, Climate Change 2022. Impacts, Adaptation and Vulnerability. Summary for Policymakers, 2022. https://www.ipcc.ch/report/ar6/wg2/.

[2] International Energy Agency, Data and Statistics, 2022. https://www.iea.org/data-and-statistics (accessed March 11, 2022).

[3] S. Biswas, D.K. Sharma, A review on the co-processing of biomass with other fuels sources, Int. J. Green. Energy 18 (2021) 793–811, https://doi.org/10.1080/15435075.2021.1880914.

[4] R.H. Perry, D.W. Green. Perry's Chemical Engineers' Handbook, 7th ed..,, McGraw-Hill,, 1999.

[5] S. Ren, H. Lei, L. Wang, Q. Bu, S. Chen, J. Wu, Thermal behaviour and kinetic study for woody biomass torrefaction and torrefied biomass pyrolysis by TGA, Biosyst. Eng. 116 (2013) 420–426, https://doi.org/10.1016/j.biosystemseng.2013.10.003.

[6] W.H. Chen, P.C. Kuo, Isothermal torrefaction kinetics of hemicellulose, cellulose, lignin and xylan using thermogravimetric analysis, Energy 36 (2011) 6451–6460, https://doi.org/10.1016/j.energy.2011.09.022.

[7] N. Brojolall, D. Surroop, Improving fuel characteristics through torrefaction, Energy 246 (2022) 123359, https://doi.org/10.1016/j.energy.2022.123359.

[8] I. Abdullah, N. Ahmad, M. Hussain, A. Ahmed, U. Ahmed, Y.K. Park, Conversion of biomass blends (walnut shell and pearl millet) for the production of solid biofuel via torrefaction under different conditions, Chemosphere 295 (2022) 133894, https://doi.org/10.1016/j.chemosphere.2022.133894.

[9] A. Cardarelli, S. Pinzi, M. Barbanera, Effect of torrefaction temperature on spent coffee grounds thermal behaviour and kinetics, Renew. Energy 185 (2022) 704–716, https://doi.org/10.1016/j.renene.2021.12.116.

[10] T.R. Sarker, S. Nanda, A.K. Dalai, V. Meda, A Review of Torrefaction Technology for Upgrading Lignocellulosic Biomass to Solid Biofuels, BioEnergy Res 14 (2021) 645–669, https://doi.org/10.1007/s12155-020-10236-2.

[11] E. Atanes, A. Nieto-Márquez, A. Cambra, M.C. Ruiz-Pérez, F. Fernández-Martínez, Adsorption of SO2 onto waste cork powder-derived activated carbons, Chem. Eng. J. 211–212 (2012) 60–67, https://doi.org/10.1016/j.cej.2012.09.043.

[12] A.U. Şen, C. Nobre, L. Durão, I. Miranda, H. Pereira, M. Gonçalves, Low-temperature biochars from cork-rich and phloem-rich wastes: fuel, leaching, and methylene blue adsorption properties, Biomass-.-. Convers. Biorefinery. (2020), https://doi.org/10.1007/s13399-020-00949-x.

[13] C. Nobre, A. Şen, L. Durão, I. Miranda, H. Pereira, M. Gonçalves, Low-temperature pyrolysis products of waste cork and lignocellulosic biomass: product characterization, Biomass-.-. Convers. Biorefinery. (2021), https://doi.org/10.1007/s13399-021-01300-8.

[14] J.Y. Lee, H.W. Lee, Y.M. Kim, Y.K. Park, The effect of biomass torrefaction on the catalytic pyrolysis of Korean cork oak, Appl, Chem. Eng. 29 (2018) 350–355, https://doi.org/10.14478/ace.2018.1050.

[15] D.C. Montgomery, Design and Analysis of Experiments, John Wiley and Sons,, New York, 2001.

[16] P.D. Valera-Medina, A.M. Lopez-Reyes, Critical analysis of 2k factorial design based on applied cases, Sci. Tech. (2011) 101–106.

[17] C. Buratti, M. Barbanera, E. Lascaro, F. Cotana, Optimization of torrefaction conditions of coffee industry residues using desirability function approach, Waste Manag 73 (2018) 523–534, https://doi.org/10.1016/j.wasman.2017.04.012.

[18] R.K. Singh, A. Sarkar, J.P. Chakraborty, Effect of torrefaction on the physicochemical properties of pigeon pea stalk (Cajanus cajan) and estimation of kinetic parameters, Renew. Energy 138 (2019) 805–819, https://doi.org/10.1016/j.renene.2019.02.022.

[19] G. Derringer, R. Suich, Simultaneous Optimization of Several Response Variables, J. Qual. Technol. 12 (1980) 214–219, https://doi.org/10.1080/00224065.1980.11980968.

[20] TA-Instruments, Thermal Analysis Applications Brief. Proximate Analysis of Coal and Coke. Number TA-129., n.d. https://www.tainstruments.com/applications-library-search/.

[21] AENOR, UNE-EN ISO 18122:2016 Biocombustibles sólidos. Determinación del contenido de ceniza, (2016).

[22] AENOR, UNE-EN ISO 18123:2016 Biocombustibles sólidos. Determinación del contenido en materia volátil, (2016).

[23] AENOR, UNE-EN ISO 18134–3:2016 Biocombustibles sólidos. Determinación del contenido de humedad. Método de secado en estufa. Parte 3: humedad de la muestra para análisis general, (2016).

[24] S. Gent, M. Twedt, C. Gerometta, E. Almberg, Fundamental Theories of Torrefaction by Thermochemical Conversion. in: Theor. Appl. Asp. Biomass Torrefaction, Elsevier,, 2017, pp. 41–75, https://doi.org/10.1016/b978-0-12-809483-9.00003-8.

[25] J. Parikh, S.A. Channiwala, G.K. Ghosal, A correlation for calculating HHV from proximate analysis of solid fuels, Fuel 84 (2005) 487–494, https://doi.org/10.1016/j.fuel.2004.10.010.

[26] Y. Niu, Y. Lv, Y. Lei, S. Liu, Y. Liang, D. Wang, S. Hui, Biomass torrefaction: properties, applications, challenges, and economy, Renew. Sustain. Energy Rev. 115 (2019) 18, https://doi.org/10.1016/j.rser.2019.109395.

[27] R. Barzegar, A. Yozgatligil, H. Olgun, A.T. Atimtay, TGA and kinetic study of different torrefaction conditions of wood biomass under air and oxy-fuel combustion atmospheres, J. Energy Inst. (2019), https://doi.org/10.1016/j.joei.2019.08.001.

[28] A.M. Ribeiro, E. Ramalho, M.P. Neto, R.M. Pilão, Thermogravimetric analysis of high-density cork granules using isoconversional methods, Energy Rep. 8 (2022) 442–447, https://doi.org/10.1016/j.egyr.2022.01.100.

[29] U. Şen, H. Pereira, Pyrolysis behavior of alternative cork species, J. Therm. Anal. Calorim. 147 (2022) 4017–4025, https://doi.org/10.1007/s10973-021-10844-w.

[30] E. Kethobile, C. Ketlogetswe, J. Gandure, Torrefaction of non - oil Jatropha curcas L. (Jatropha) biomass for solid fuel, Heliyon 6 (2020) e05657, https://doi.org/10.1016/j.heliyon.2020.e05657.

[31] J. Fu, S. Summers, S.Q. Turn, W. Kusch, Upgraded pongamia pod via torrefaction for the production of bioenergy, Fuel 291 (2021) 120260, https://doi.org/10.1016/j.fuel.2021.120260.

[32] I. Mian, X. Li, Y. Jian, O.D. Dacres, M. Zhong, J. Liu, F. Ma, N. Rahman, Kinetic study of biomass pellet pyrolysis by using distributed activation energy model and Coats Redfern methods and their comparison, Bioresour. Technol. 294 (2019) 122099, https://doi.org/10.1016/j.biortech.2019.122099.

[33] G. San Miguel, F. Gutiérrez, Tecnologías para el uso y transformación de biomasa energética, Mundiprensa, 2015.
[34] B. Cui, Z. Chen, D. Guo, Y. Liu, Investigations on the pyrolysis of microalgal-bacterial granular sludge: Products, kinetics, and potential mechanisms, Bioresour. Technol. 349 (2022) 126328, https://doi.org/10.1016/j.biortech.2021.126328.
[35] Q. Wang, D. Chu, C. Luo, Z. Lai, S. Shang, S. Rahimi, J. Mu, Transformation mechanism from cork into honeycomb–like biochar with rich hierarchical pore structure during slow pyrolysis, Ind. Crops Prod. 181 (2022) 114827, https://doi.org/10.1016/j.indcrop.2022.114827.
[36] M.H. Lopes, A.S. Barros, C. Pascoal Neto, D. Rutledge, I. Delgadillo, A.M. Gil, Variability of cork from portuguese Quercus suber studied by solid-state 13C NMR and FTIR spectroscopies, Biopolym. - Biospectroscopy Sect. 62 (2001) 268–277, https://doi.org/10.1002/bip.1022.
[37] G. Blázquez, A. Pérez, I. Iáñez-Rodríguez, C. Martínez-García, M. Calero, Study of the kinetic parameters of thermal and oxidative degradation of various residual materials, Biomass-.-. Bioenergy 124 (2019) 13–24, https://doi.org/10.1016/j.biombioe.2019.03.008.
[38] F. Xu, D. Wang, Analysis of Lignocellulosic Biomass Using Infrared Methodology. in: Pretreat. Biomass, Elsevier,, 2015, pp. 7–25, https://doi.org/10.1016/B978-0-12-800080-9.00002-5.
[39] U. Sen, M. Martins, E. Santos, M.A. Lemos, F. Lemos, H. Pereira, Slow Pyrolysis of Quercus cerris Cork: Characterization of Biochars and Pyrolysis Volatiles, Environ. - Mdpi. 10 (2023) 1–14, https://doi.org/10.3390/environments10010004.
[40] K. Krysanova, A. Krylova, M. Kulikova, A. Kulikov, O. Rusakova, Biochar characteristics produced via hydrothermal carbonization and torrefaction of peat and sawdust, Fuel 328 (2022) 125220, https://doi.org/10.1016/j.fuel.2022.125220.
[41] A.N. Dias, V. Simão, J. Merib, E. Carasek, Cork as a new (green) coating for solid-phase microextraction: Determination of polycyclic aromatic hydrocarbons in water samples by gas chromatography-mass spectrometry, Anal. Chim. Acta 772 (2013) 33–39, https://doi.org/10.1016/j.aca.2013.02.021.
[42] M. Wzorek, R. Junga, E. Yilmaz, P. Niemiec, Combustion behavior and mechanical properties of pellets derived from blends of animal manure and lignocellulosic biomass, J. Environ. Manag. 290 (2021) 112487, https://doi.org/10.1016/j.jenvman.2021.112487.
[43] S.T. Farrow, C. Sun, H. Liu, K. Le Manquais, C.E. Snape, Comparative study of the inherent combustion reactivity of sawdust chars produced by TGA and in the drop tube furnace, Fuel Process. Technol. 201 (2020) 106361, https://doi.org/10.1016/j.fuproc.2020.106361.